

The Synthesis of CdTe by Means of Fused Salt Electrolysis and Its Characterization

Hideki MINOURA,* Masakazu KITAKATA, Takashi SUGIURA, Minoru MURAYAMA,
and Yasusada UENO

Department of Synthetic Chemistry, Faculty of Engineering, Gifu University,
1-1 Yanagido, Gifu 501-11

(Received December 22, 1986)

Crystalline cadmium telluride layers of a cubic structure have been deposited potentiostatically on graphite cathodes by means of fused salt electrolysis employing CdCl_2 and $\text{TeO}_2/\text{Na}_2\text{TeO}_3$ in an LiCl-KCl eutectic melt at 450°C . X-Ray diffraction and scanning-electron-microscope studies show that (i) these layers have a tendency to grow with a preferred orientation along the $\langle 111 \rangle$ direction and (ii) the surface morphology changes drastically with the change in the applied potential. Voltammetric analyses indicate two distinct mechanisms for cadmium telluride deposition; one is the codeposition of cadmium and tellurium occurring at potentials more negative than $-0.2\text{ V (vs. Ag/AgCl)}$, and the other is the ionic reaction of the cathodically formed telluride ion with the cadmium ion occurring at potentials more negative than $-0.7\text{ V (vs. Ag/AgCl)}$. As-deposited crystals are either n- or p-type, depending on the melt composition and the applied potential.

The electrodeposition from fused salts seems to be one of most promising of the new methods of obtaining semiconductor films. The important merits of this method are as follows; (i) it is easy to control the deposition conditions, as is common in the case of electrochemical deposition methods, and (ii) it enables us to obtain compound semiconductors with a high crystallinity since the deposition takes place at a relatively high temperature compared to that of aqueous solutions. In spite of its usefulness, however, no systematic studies of the preparation of semiconductor materials by means of fused salt electrolysis have been reported thus far, although a few reports dealing inadequately with this subject are available in the literature.^{1–5} In the past decade our laboratory has been engaged in a major effort to produce polycrystalline cadmium chalcogenide films/layers by employing various methods aimed at their efficient use in photoelectrochemical cells.⁶ As a part of this series of investigations, we have already reported the crystal growth of CdSe by means of fused salt electrolysis and its applicability in a photoelectrochemical cell.^{7,8}

This paper deals with the electrodeposition of CdTe by means of fused salt electrolysis. CdTe is a promising material for solar photovoltaic devices because it possesses a direct bandgap of 1.44 eV , which is close to the maximum of the solar spectrum, and because it has a high absorption coefficient. Besides, with it both n-type and p-type forms can be conveniently prepared. Actually, polycrystalline CdTe has already been successfully used in a CdS/CdTe heterojunction solar cell for commercial use by Matsushita's group.⁹ The electrodeposition of CdTe films from an aqueous solution and a nonaqueous solution has already been reported.^{10–13} Electrodeposition is a low-temperature process (usually a room-temperature process) without resort to any vacuum technology and is subject to minimum losses of materials; thus, it offers a convenient and inexpensive method of film fabrication.

However, as-deposited films obtained by this method generally have a poor crystallinity, a subsequent heat-treatment is required for its use in a photovoltaic device. In this particular aspect, the electrodeposition from fused salt has the advantage that no such subsequent heat-treatment is required because of the simultaneous occurrence of the electrodeposition and the crystal growth.

In this paper, the mechanism of CdTe deposition by means of fused salt electrolysis will be proposed on the basis of the previously proposed mechanism for the similarly deposited CdSe. We have also examined the possibility of getting n- and p-type samples of CdTe selectively by changing the deposition conditions, namely, the electrolytic potential and the salt composition.

Experimental

The experimental apparatus and procedures are nearly the same as those described in a previous paper.⁷

Almost all the electrodeposition procedures from the fused salts thus far reported have been carried out under galvanostatic condition in a two-electrode configuration.^{1–4} In order to carry out the potentiostatic electrolysis, we adopted a three-electrode system consisting of a graphite working electrode (a substrate onto which CdTe is deposited), a graphite counter electrode, and an Ag/AgCl reference electrode. The potentiostatic electrolysis is required to examine the potential-dependent deposition, as has been emphasized earlier in the case of CdSe.⁸ All the potential values in the present paper are expressed with respect to this reference electrode.

CdCl_2 and $\text{Na}_2\text{TeO}_3/\text{TeO}_2$ were added to the LiCl-KCl electrolyte of the eutectic composition as the source materials of cadmium and tellurium respectively. Electrolyses were carried out at 450°C .

The crystal structure and the morphology of the deposits were examined by means of an X-ray diffractometer (Rigaku Denki) and a scanning electron microscope (Hitachi H-8010) respectively.

To determine the type of the majority carrier, the current-potential curves under illumination were recorded for the deposits in an aqueous sulfide solution.

Results and Discussion

According to our preliminary experiments, CdTe has been found to be deposited by electrolysis in the melts containing CdCl_2 and TeO_2 at the bath temperature of 450°C . Therefore, prior to the analysis of the CdTe deposition reaction, the cathodic polarization curves of a cadmium-source material and tellurium-source materials have been examined separately in order to understand the CdTe deposition mechanism by using the same method as was reported previously for CdSe.⁹⁾ The results on the voltammetric curves of a cadmium source will be omitted in the present paper, as they have already been reported in a previous paper.⁹⁾

Reduction of Te(+4). A voltammetric curve under cathodic polarization in Na_2TeO_3 -containing melts is shown in Fig. 1. A cathodic current starts to flow at $+0.2\text{ V}$, reaches the saturation value at -0.3 V , and rises again at -0.7 V . The deposit obtained at the first wave exhibits a metallic gray color and was identified as a metallic tellurium by means of the X-ray diffraction data. It has been noticed that, when polarized more cathodically than -0.7 V , the deposit on the substrate gradually disappears. These results indicate that the deposition of a metallic tellurium takes place at the first cathodic wave, while the further reduction of the metallic Te to $\text{Te}(-2)$ proceeds at the second cathodic wave, analogous to the reduction of $\text{Se}(+4)$ reported in the previous paper.⁹⁾ Bodewig and Plambeck¹⁵⁾ examined the electrochemical behavior of a tellurium electrode in the fused LiCl-KCl eutectic and reported the formation of a stable lithium-tellurium intermetallic compound, i.e., Li_2Te , at -0.67 V . However, we could not detect such an intermetallic compound in our X-ray diffractograms. This particular result can perhaps be attributed to the difference in the electrodes used, i.e., a tellurium electrode in their work and a tellurium-deposited graphite electrode in our work.

In order to understand what reactions are taking

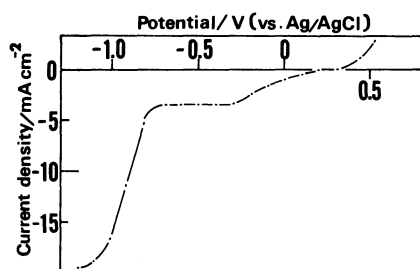


Fig. 1. Voltammogram for the reduction of Na_2TeO_3 . Concentration of Na_2TeO_3 is $1.2 \times 10^{-2}\text{ mol\%}$.

place in the second-wave reduction process, cyclic voltammetric experiments were performed in the potential range between -0.6 and -0.9 V . Figure 2 shows cyclic voltammograms with different sweep rates. The peak potential is independent of the sweep rate within our experimental sweep rate range, and the oxidation-peak height is smaller than the reduction-peak height. The peak current density is proportional to the square root of the potential sweep rate and the concentration of Na_2TeO_3 , as is indicated in Figs. 3 and 4. It follows that the cathodic reaction occurring in the potential region is a reversible reaction involving a soluble product. From the plot

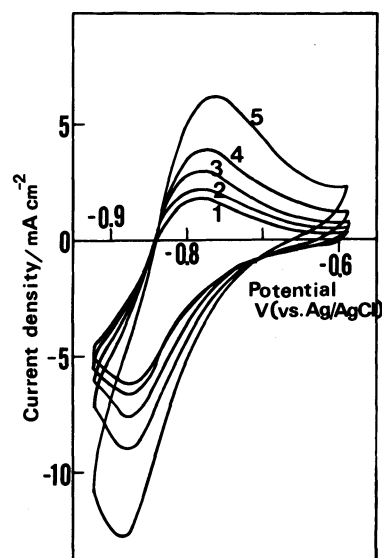


Fig. 2. Cyclic voltammograms for the reduction of Na_2TeO_3 at different sweep rates. Concentration of Na_2TeO_3 is $4.85 \times 10^{-4}\text{ mol\%}$. 1: 20 mV s^{-1} , 2: 25 mV s^{-1} , 3: 33.3 mV s^{-1} , 4: 50 mV s^{-1} , 5: 100 mV s^{-1} .

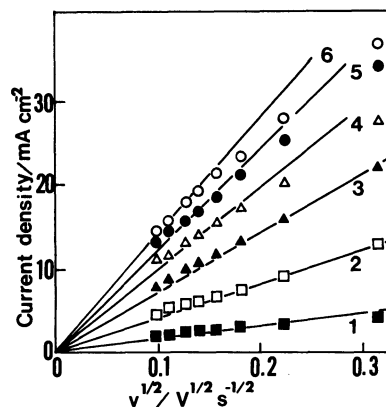


Fig. 3. Voltammetric peak current vs. square root of the sweep rate for the reduction of $\text{Te}(0)$ in $\text{LiCl}(0.236\text{ mol})$ - $\text{KCl}(0.172\text{ mol})$ melts. Quantity of Na_2TeO_3 in melts; 1: $1.01 \times 10^{-4}\text{ mol}$, 2: $1.98 \times 10^{-4}\text{ mol}$, 3: $2.99 \times 10^{-4}\text{ mol}$, 4: $3.92 \times 10^{-4}\text{ mol}$, 5: $4.96 \times 10^{-4}\text{ mol}$, 6: $5.95 \times 10^{-4}\text{ mol}$.

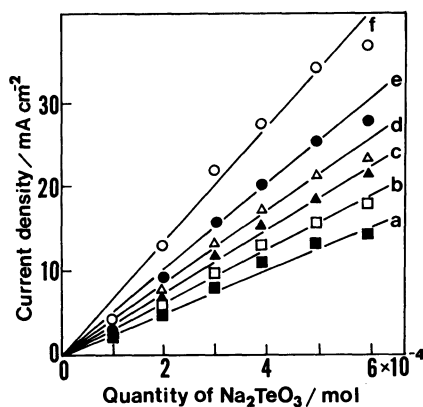


Fig. 4. Voltammetric peak current vs. Na_2TeO_3 concentration for the reduction of $\text{Te}(0)$ in $\text{LiCl}(0.236 \text{ mol})$ - $\text{KCl}(0.172 \text{ mol})$ melts. Sweep rate; a: 10 mV s^{-1} , b: 16.7 mV s^{-1} , c: 25 mV s^{-1} , d: 33.3 mV s^{-1} , e: 50 mV s^{-1} , f: 100 mV s^{-1} .

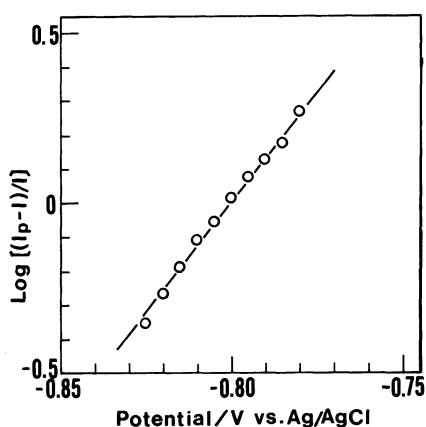
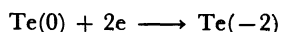


Fig. 5. Plots of $\log [(i_p - i)/i]$ vs. electrode potential for the reduction of Na_2TeO_3 . Na_2TeO_3 concentration: $4.85 \times 10^{-4} \text{ mol\%}$, Sweep rate: 16.7 mV s^{-1} .

shown in Fig. 5, and by applying Matsuda and Ayabe's equation,¹⁶⁾ the number of electrons involved in this cathodic process, n , was calculated by using the procedure reported in a previous paper.⁸⁾ This calculation yields the value of 1.89. In this way, it is confirmed that the reduction expressed as:



proceeds at potentials more negative than -0.7 V .

Almost the same behavior was observed when a TeO_2 -containing melt was used instead of an Na_2TeO_3 -containing melt, with the only exception of a small increase in the cathodic current.

Deposition of CdTe. In the melt containing both CdCl_2 as a cadmium source and Na_2TeO_3 as a tellurium-source in an equimolar composition, the cathodic current starts to flow at around $+0.2 \text{ V}$,

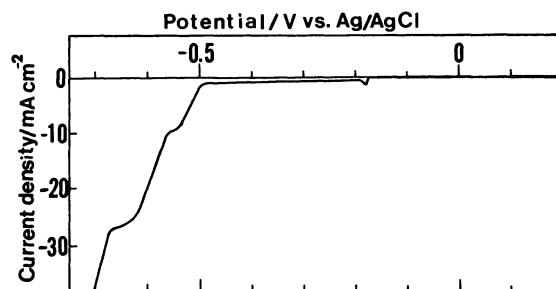


Fig. 6. Voltammograms for the deposition of CdTe in $\text{LiCl}(0.236 \text{ mol})$ - $\text{KCl}(0.172 \text{ mol})$ - $\text{CdCl}_2(0.005 \text{ mol})$ - $\text{Na}_2\text{TeO}_3(0.005 \text{ mol})$. Sweep rate: 0.1 mV s^{-1} .

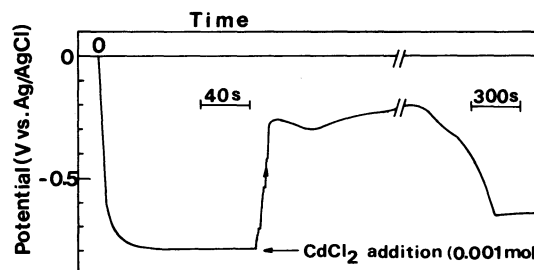


Fig. 7. Electrode potential change with time by the addition of CdCl_2 under galvanostatic electrolysis of -10 mA in $\text{LiCl}(0.236 \text{ mol})$ - $\text{KCl}(0.172 \text{ mol})$ - $\text{Na}_2\text{TeO}_3(0.005 \text{ mol})$ melt. Electrode surface area: 3.4 cm^2 .

which corresponds to the reduction of $\text{Te}(+4)$ to $\text{Te}(0)$. As is shown in the voltammogram of Fig. 6, a characteristic peak appears at about -0.2 V and the current remains constant with an increase in the cathodic polarization to -0.5 V . The CdTe deposit was observed at potentials more negative than -0.2 V . The appearance of the cathodic peak at around -0.2 V will be discussed later. The redox potential of Cd/Cd^{2+} was reported to be -0.589 V ; our result implies that the deposition of cadmium metal starts to take place at -0.59 V . A comparison of the CdTe deposition onset potential of -0.2 V with this standard redox potential of Cd/Cd^{2+} clearly shows the occurrence of the underpotential deposition of CdTe.

The small peak at around -0.2 V in the voltammogram shown in Fig. 6 can be explained by assuming that the tellurium which had been deposited at the potentials more positive than -0.2 V was changed into CdTe at -0.2 V by the incorporation of cadmium, which starts to be deposited at this potential. In order to confirm this assumption, galvanostatic measurements were performed. Figure 7 presents the potential-time curve during the galvanostatic electrolysis. As can be seen from this curve, the electrode potential changes toward negative values and reaches the stationary value of -0.8 V when a

graphite electrode is polarized cathodically in melts containing only the tellurium source. After carrying out this electrolysis for 2 minutes and adding CdCl_2 to the melt, the potential suddenly changes to about -0.2 V. This potential corresponds to the small peak in Fig. 6. It is further seen that the potential gradually shifts to more negative values and then reaches the stationary value of -0.64 V. Taking into account the small peak at -0.2 V in Fig. 6, the transition time at -0.2 V in Fig. 7 can be regarded as the time for changing the deposited tellurium to CdTe by the incorporation of the deposited cadmium metal. Therefore, this transition time probably depends on the quantity of the deposited tellurium. Actually, this idea is supported by the results shown in Figs. 7 and 8, which demonstrate that halving the electrolysis time before CdCl_2 addition (Fig. 8) results in the reduction of the transition time at -0.2 V to about one-half of

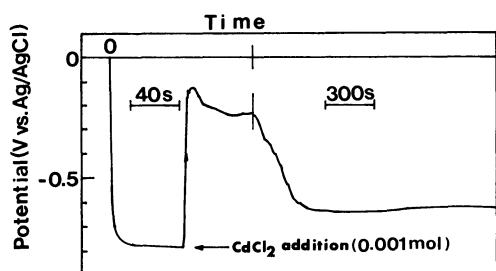


Fig. 8. Electrode potential change with time by the addition of CdCl_2 under galvanostatic electrolysis of -10 mA in $\text{LiCl}(0.236 \text{ mol})$ - $\text{KCl}(0.172 \text{ mol})$ - $\text{Na}_2\text{TeO}_3(0.005 \text{ mol})$ melt. Electrode surface area: 1.9 cm^2 . Electrolysis time before CdCl_2 is a half of that in Fig. 7.

that in Fig. 7. The corresponding peak was not observed in the case of CdSe deposition, although a similar process can be expected to occur. This difference is attributable to the difference in the melting points of selenium (220.2°C) and tellurium (449.8°C). As the deposited selenium is in a liquified state, it is unlikely to stick to the graphite substrate.

The observation that the cathodic current rises again at -0.59 V suggests the occurrence of a usual cadmium deposition together with the above-mentioned underpotential deposition. The increase in the cathodic current at -0.7 V may be due to the reduction of $\text{Te}(0)$ or $\text{Te}(+4)$ to $\text{Te}(-2)$. Thus, CdTe formation by a reaction of Te^{2-} with Cd^{2+} in the melt should take place in addition to the above-mentioned codeposition. Therefore, the deposition reactions at various potentials can be summarized in the manner shown in Fig. 9.

To get further information on the CdTe deposition process, the change in the surface morphology as the electrolysis progressed was monitored by means of a

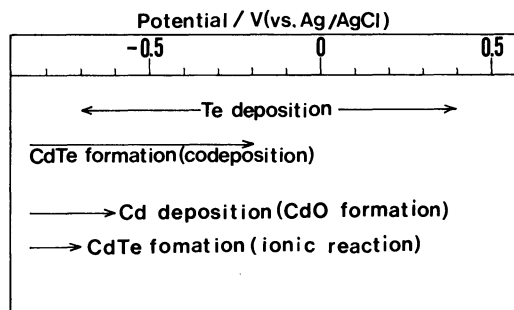
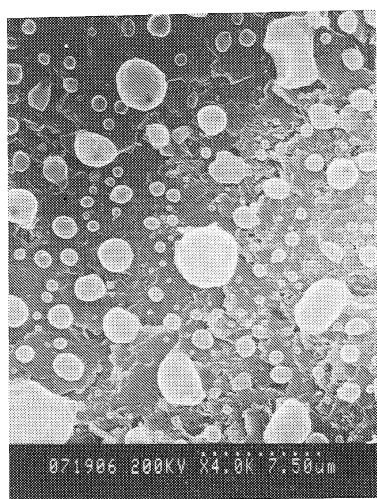
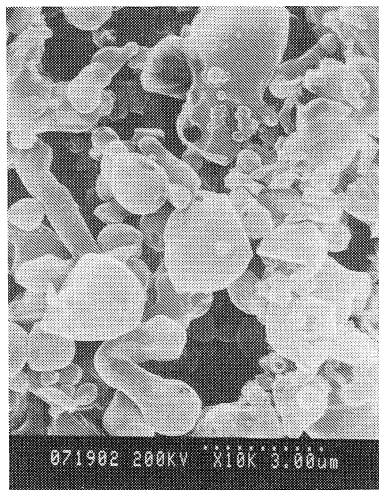


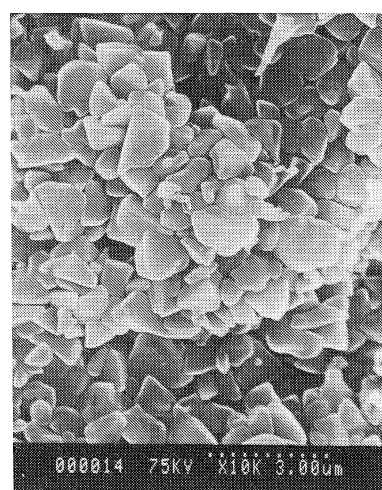
Fig. 9. Deposition reactions at different electrolytic potentials.



A



B

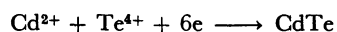


C

Fig. 10. SEM micrographs of the deposits obtained at -0.6 V. Quantity of electricity passed during electrodeposition; (A) 1.3 C cm^{-2} , (B) 1.3 C cm^{-2} , (C) 2.5 C cm^{-2} . (B) is a different place from (A) in the same sample.

scanning electron microscope. Figure 10 presents SEM micrographs of the deposits obtained at various stages of the electrolysis carried out at -0.6 V. Initially, spherical-shaped deposits appeared, as is shown in Fig. 10 (A). The EPMA results revealed that these deposits are metallic tellurium. This characteristic morphology becomes quite obvious if we consider the fact that the bath temperature is nearly the same as the melting point of tellurium. With the increase in the amount of electricity passed through, other deposits, but with a linear edge in contrast to the above-mentioned spherical-shaped ones, appear, as is shown in Fig. 10 (C). These deposits were identified as CdTe by means of the X-ray diffractograms and the EPMA results. The corresponding photographs show that tellurium is first deposited onto the substrate, and then cadmium is deposited and incorporated into tellurium deposits, resulting in CdTe formation. Thus, our SEM data further support the above-mentioned mechanism of CdTe codeposition.

Figure 11 shows the relationship between the weight gain and the amount of electricity passed through during fused salt electrolysis at -0.6 V. It is clear from these results that the weight of the deposits is directly proportional to the amount of electricity passed through; in other words, the current efficiency remains nearly constant during the electrolysis. Assuming that the overall reaction for CdTe deposition is expressed as:



the apparent current efficiency estimated on the basis of Faraday's law, is 43%. Such a low current efficiency may be attributable to a falling down of some

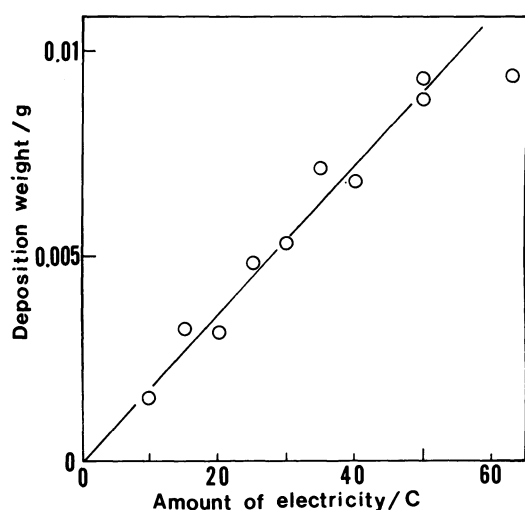


Fig. 11. Deposition weight vs. amount of electricity during electrodeposition from $\text{LiCl}(0.236 \text{ mol})\text{-KCl}(0.172 \text{ mol})\text{-CdCl}_2(0.005 \text{ mol})\text{-Na}_2\text{TeO}_3(0.005 \text{ mol})$ melt at -0.7 V.

deposited material while the cathode was dipped in a 1% HCl solution after electrolysis. This dipping procedure was employed to remove the solvents and solutes stuck to the deposits. Therefore, we feel that the real current efficiency must be higher than 43%.

Characterization of the Deposits. X-Ray diffractograms of the deposits obtained at the electrolytic potentials of -0.4 and -0.7 V are shown in Fig. 12. All these peaks match well with the ASTM data of cubic CdTe (zinc blende type). In the diffractograms of the deposit at $-0.4\text{--}0.6$ V, there are some prominent peaks due to CdTe, the intensities of which are in good agreement with the standard powder diffraction data for CdTe. Interestingly, in the diffractogram of the deposits obtained at -0.7 V, only one strong peak corresponding to the (111) plane appears; it is indicative of the crystal growth with a preferred orientation along the $\langle 111 \rangle$ direction. This can be ascribed to a relatively high deposition rate at -0.7 V, in which the preferential growth of crystal nuclei with the most stable (111) plane may proceed.

We determined the conductivity type of our deposits by studying the current-potential curves under illumination in an aqueous solution. The deposit which exhibits an anodic photocurrent is referred to as the n-type, while that which exhibits a cathodic

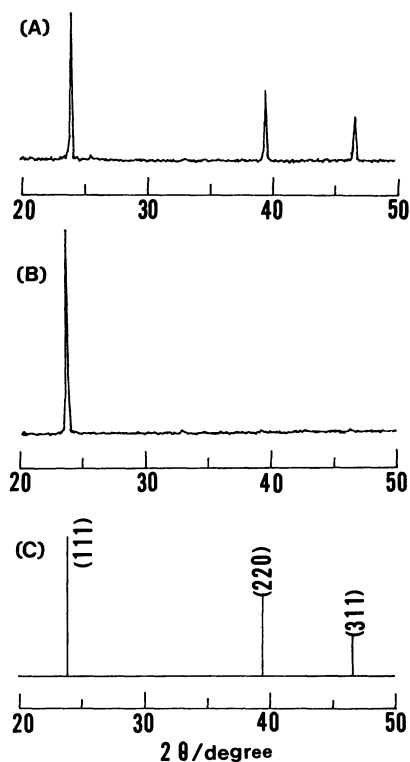


Fig. 12. X-Ray diffraction patterns of the deposits obtained from $\text{LiCl}(0.236 \text{ mol})\text{-KCl}(0.172 \text{ mol})\text{-CdCl}_2(0.005 \text{ mol})\text{-Na}_2\text{TeO}_3(0.005 \text{ mol})$ melt. Deposition potential; (A) -0.4 V, (B) -0.7 V. (C) is the ASTM data for cubic CdTe.

photocurrent is referred to as the p-type, in the present paper.

Table 1 summarizes the electrical-conduction type as well as the chemical composition of the deposits obtained under various melt compositions and electrolytic potentials. The chemical compositions correspond to those estimated by means of X-ray diffractograms of the deposits.

From the melt with equimolar CdCl_2 and TeO_2 , both n-type and p-type CdTe were obtained. At -0.1 V, no CdTe was deposited, however; only metallic tellurium was detected. At potentials more negative than -0.2 V, CdTe was deposited. It should be noted that both n-type and p-type are obtained by controlling the electrolytic potential applied. At potentials more negative than -0.6 V, only n-type CdTe was obtained. This interesting result seems quite reasonable if we consider that -0.59 V is the potential at which cadmium deposition starts to occur and that the n-type is associated principally with an excess of cadmium.

From the melt containing an excess of CdCl_2 , an n-type sample is more likely to be deposited. Some weak peaks which can be assigned to CdO were found in the X-ray diffractograms. This indicates that a

further excess of cadmium leads to the CdO formation. On the other hand, from a melt with an excess of a tellurium source, a p-type sample was found to be deposited, even at -0.7 V. In this case, the deposits were found to contain metallic tellurium, whereas no CdO was detectable. This is attributable to the slower rate of the deposition of cadmium compared to that of tellurium. Such an excess of tellurium in the deposits can be removed by subsequent heat-treatment, as has been reported in the case of CdTe films deposited from an aqueous solution.¹³⁾ These results are consistent with the above consideration of the deposition reaction.

When we add Na_2TeO_3 instead of TeO_2 as a tellurium-source material, an n-type is more likely to be deposited. This is attributable to a smaller cathodic current caused by a tellurium deposition, as was mentioned above.

Figure 13 displays SEM micrographs of the deposits obtained at various electrolytic potentials from KCl-LiCl melts containing 0.005 mol CdCl_2 and 0.005 mol Na_2TeO_3 . As can clearly be seen from these photographs, the deposits at -0.4 — -0.6 V have similar morphologies with tetrahedron-shaped crystals. However, it is interesting to note that, with the

Table 1. Chemical Composition of the Deposits under Various Conditions in LiCl (0.236 mol)-KCl (0.172 mol) Melts

Melt composition $\frac{\text{CdCl}_2}{\text{mol}}$	$\frac{\text{TeO}_2}{\text{mol}}$	Deposition potential V vs. Ag/AgCl	Cathode product ^{a)}			Photocurrent ^{b)}
			CdTe	Te	CdO	
0.0067	0.0033	-0.1	—	W	—	—
0.0067	0.0033	-0.2	VS	W	—	p, (n)
0.0067	0.0033	-0.3	VS	W	—	p
0.0067	0.0033	-0.4	VS	—	—	p, (n)
0.0067	0.0033	-0.5	M	W	W	n, (p)
0.0067	0.0033	-0.6	W	—	W	n
0.0067	0.0033	-0.7	W	—	M	n
0.0067	0.0033	-0.8	W	—	W	n
0.0067	0.0033	-0.9	W	—	W	n
0.005	0.005	-0.1	—	M	—	—
0.005	0.005	-0.2	S	W	—	p
0.005	0.005	-0.3	M	—	—	p
0.005	0.005	-0.4	S	—	—	p
0.005	0.005	-0.5	S	—	—	p
0.005	0.005	-0.6	M	W	—	n
0.005	0.005	-0.7	M	VW	—	n
0.0033	0.0067	-0.2	M	M	—	p
0.0033	0.0067	-0.3	M	W	—	p
0.0033	0.0067	-0.4	M	W	—	p
0.0033	0.0067	-0.5	M	VW	—	p
0.0033	0.0067	-0.6	S	—	—	p
0.0033	0.0067	-0.7	W	W	—	p

The amount of electricity consumed during electrodeposition is 20 C cm^{-2} . a) Estimated from X-ray diffractograms: VS, very strong, S, strong, M, medium, W, weak, VW, very weak, —, undetectable. b) A deposit which shows an anodic photoresponse is termed "n", while that which shows a cathodic photoresponse is termed "p". When a deposit exhibits both anodic and cathodic photoresponses, the weaker one is shown in parentheses.

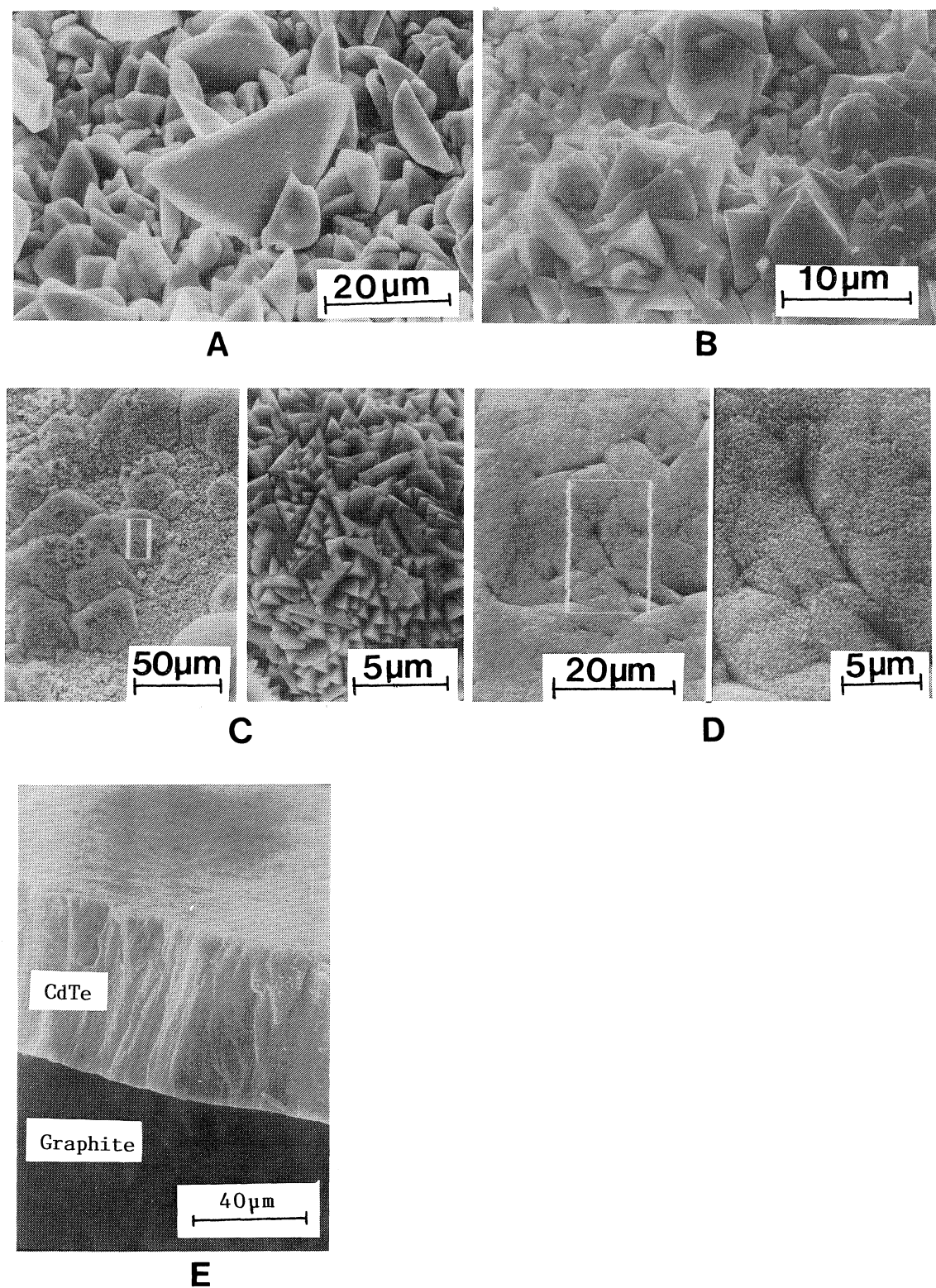


Fig. 13. SEM micrographs of the deposits obtained at different electrolytic potentials from $\text{LiCl}(0.236 \text{ mol})\text{-KCl}(0.172 \text{ mol})\text{-CdCl}_2(0.005 \text{ mol})\text{-Na}_2\text{TeO}_3(0.005 \text{ mol})$ melt. Deposition potential; (A) -0.4 V , (B) -0.5 V , (C) -0.6 V , (D) -0.7 V . (E) is the cross section picture of the deposit obtained at -0.7 V .

more negative potentials, smaller crystals are deposited. The size of one crystal is 10–50 μm when deposited at -0.4 V , 5–10 μm at -0.5 V , and about 1 μm at -0.6 V . The deposits at -0.7 V have a slightly different morphology which seems to consist of very fine grains. Figure 13(E) shows a cross-section of the deposit at -0.7 V . The deposit has a columnar structure and a comparatively uniform thickness. We can conclude from this morphology that when a uniform coating of CdTe is required, -0.7 V is the optimum electrolytic potential. Deposition at less negative potentials, in contrast, may be useful for getting a single crystal of CdTe. A further study along these lines is now in progress.

This work was supported by a Grant-in-Aid for Energy Research No. 60045054 from the Ministry of Education, Science and Culture.

References

- 1) J. J. Cuomo and R. J. Gambino, *J. Electrochem. Soc.*, **115**, 755 (1967).
- 2) A. Yamamoto and M. Yamaguchi, *Jpn. J. Appl. Phys.*, **14**, 561 (1975).
- 3) I. Markov and M. Ilieva, *Thin Solid Films*, **74**, 109 (1980).
- 4) L. F. Schneemeyer and U. Cohen, *J. Electrochem. Soc.*, **130**, 1530 (1983).
- 5) R. Boen and J. Bouteillon, *J. Appl. Electrochem.*, **13**, 277 (1983).
- 6) H. Minoura, M. Tsuiki, and T. Oki, *Ber. Bunsenges. Phys. Chem.*, **81**, 588 (1977); M. Tsuiki, H. Minoura, T. Nakamura, and Y. Ueno, *J. Appl. Electrochem.*, **8**, 523 (1978); M. Tsuiki, Y. Ueno, T. Nakamura, and H. Minoura, *Chem. Lett.*, **1978**, 289; H. Minoura, K. Kobayashi, Y. Ueno, and M. Tsuiki, *Chem. Lett.*, **1982**, 505; Y. Ueno, H. Minoura, T. Nishikawa, and M. Tsuiki, *J. Electrochem. Soc.*, **130**, 43 (1983).
- 7) H. Minoura, T. Negoro, M. Kitakata, and Y. Ueno, *Solar Energy Mater.*, **12**, 335 (1985).
- 8) H. Minoura, T. Negoro, M. Kitakata, and Y. Ueno, *Thin Solid Films*, **147**, 65 (1987).
- 9) H. Uda, A. Nakano, K. Kuribayashi, Y. Komatsu, H. Matsumoto, and S. Ikegami, *Jpn. J. Appl. Phys.*, **22**, 1822 (1983); H. Matsumoto, K. Kuribayashi, H. Uda, Y. Komatsu, A. Nakano, and S. Ikegami, *Solar Cells*, **11**, 367 (1984).
- 10) M. P. R. Panicker, M. Knaster, and F. A. Kroeger, *J. Electrochem. Soc.*, **125**, 566 (1978).
- 11) H. J. Gerritsen, *J. Electrochem. Soc.*, **131**, 136 (1984).
- 12) R. N. Bhattacharya and K. Rajeshwar, *J. Electrochem. Soc.*, **131**, 2032 (1984).
- 13) K. Uosaki, M. Takahashi, and H. Kita, *Electrochim. Acta*, **29**, 279 (1984); M. Takahashi, K. Uosaki, and H. Kita, *J. Appl. Phys.*, **55**, 3879 (1984); *J. Electrochem. Soc.*, **131**, 2304 (1984).
- 14) A. Darkowski and M. Cocivera, *J. Electrochem. Soc.*, **132**, 2768 (1985).
- 15) F. G. Bodewig and J. A. Plambeck, *J. Electrochem. Soc.*, **117**, 618 (1970).
- 16) H. Matsuda and Y. Ayabe, *Z. Elektrochem.*, **59**, 494 (1955).